

Comparing Graph Spectra of Adjacency and Laplacian Matrices

J. F. Lutzeyer & A. T. Walden

Abstract—Typically, graph structures are represented by one of three different matrices: the adjacency matrix, the unnormalised and the normalised graph Laplacian matrices. The spectral (eigenvalue) properties of these different matrices are compared. For each pair, the comparison is made by applying an affine transformation to one of them, which enables comparison whilst preserving certain key properties such as normalised eigengaps. Bounds are given on the eigenvalue differences thus found, which depend on the minimum and maximum degree of the graph. The monotonicity of the bounds and the structure of the graphs are related. The bounds on a real social network graph, and on three model graphs, are illustrated and analysed. The methodology is extended to provide bounds on normalised eigengap differences which again turn out to be in terms of the graph’s degree extremes. It is found that if the degree extreme difference is large, different choices of representation matrix may give rise to disparate inference drawn from graph signal processing algorithms; smaller degree extreme differences result in consistent inference, whatever the choice of representation matrix. The different inference drawn from signal processing algorithms is visualised using the spectral clustering algorithm on the three representation matrices corresponding to a model graph and a real social network graph.

Index Terms—adjacency matrix, affine transformation, graph Laplacian, spectrum, graph signal processing, degree difference

I. INTRODUCTION

Graph structures are usually represented by one of three different matrices: the adjacency matrix, and unnormalised and normalised graph Laplacian matrices. We will refer to these three matrices as representation matrices. In recent years there has been an increasing interest in the use of graph structures for modelling purposes and their analysis. An overview of the numerous advances in the area of signal processing on graphs is provided in [14]. [7] contains a vast bibliography and overview of the applications of graph spectra in engineering, computer science, mathematics and other areas. [13] address the big data topic in the context of graph structures by introducing different product graphs and showing how discrete signal processing is sped up by utilising the product graph structure.

In a particular analysis, given a choice of one representation matrix, the spectral (eigenvalue) properties of the matrix are often utilised as in, for example, the spectral clustering

algorithm [17] and graph wavelets [15]. Spectral clustering has had a big impact in the recent analysis of graphs, with active research on the theoretical guarantees which can be given for a clustering determined in this way ([11],[12]). [15] use their construction of graph wavelets, utilising both the spectrum and the eigenvectors in their design, to obtain clusters on several different scales.

The different representation matrices are well established in the literature. A shifted version of the symmetric normalised graph Laplacian is used in the analysis by [12]. [14] work with the unnormalised graph Laplacian L and remark on both normalised graph Laplacians L_{rw} and L_{sym} , while [13] use the adjacency matrix A and remark on the unnormalised graph Laplacian L . [15] use the symmetric normalised graph Laplacian L_{sym} in the construction of their graph wavelets. [11] perform their analysis using the adjacency matrix A and mention the extension of their results to the graph Laplacian as future work. The question of what would have happened if another representation had been chosen instead, arises naturally when reading the networks and graph literature. The purpose of this paper is to compare the spectral properties of these different matrices, to try to gain some insight into this issue.

Our approach is to firstly apply an affine transformation to one of the matrices, before making the comparison. The transformation preserves certain key properties, such as normalized eigengaps (differences between successive eigenvalues) and the ordering of eigenvalues.

Consider a graph $G = (V, E)$ with vertex set V , where $|V| = n$, and edge set E . We will assume our graphs to be undirected and simple. An edge between vertices v_i and v_j has edge weight w_{ij} , which is defined to be 0 if there exists no edge between v_i and v_j . If the edge weights are binary, then the graph is said to be unweighted, otherwise it is a weighted graph. The matrix holding the edge weights is the adjacency matrix $A \in [0, 1]^{n \times n}$ of a graph and is defined to have entries $A_{ij} = w_{ij}$, (the maximal weight of an edge, unity, can be achieved by normalising by the maximal edge weight if necessary). The adjacency matrix is one of the standard graph representation matrices considered here.

The degree d_i of the i^{th} vertex is defined to be the sum of the weights of all edges connecting this vertex with others, i.e., $d_i = \sum_{j=1}^n w_{ij}$ and the degree matrix D is defined to be the diagonal matrix $D = \text{diag}(d_1, \dots, d_n)$. The degree sequence is the set of vertex degrees $\{d_1, \dots, d_n\}$. The minimal and maximal degree in the degree sequence is denoted d_{\min} and d_{\max} , respectively. (An important special case is that of d -regular graphs, in which each vertex is of degree d , so that

Copyright (c) 2017 IEEE. Personal use of this material is permitted. However, permission to use this material for any other purposes must be obtained from the IEEE by sending a request to pubs-permissions@ieee.org. Johannes Lutzeyer and Andrew Walden are both at the Department of Mathematics, Imperial College London, 180 Queen’s Gate, London SW7 2AZ, UK. (e-mail: johannes.lutzeyer11@imperial.ac.uk and a.walden@imperial.ac.uk).

$d_{\max} = d_{\min} = d$, and the degree matrix is a scalar multiple of the identity matrix, $D = dI$, where I is the identity matrix.)

For a general D matrix, the unnormalised graph Laplacian, L , is defined as

$$L = D - A.$$

In the literature there are two normalised Laplacians which are considered [17]; these follow from the unnormalised graph Laplacian by use of the inverse of the degree matrix as follows:

$$L_{rw} = D^{-1}L; \quad L_{sym} = D^{-1/2}LD^{-1/2}. \quad (1)$$

Since they are related by a similarity transform the sets of eigenvalues of these two normalised Laplacians are identical and we only need to concern ourselves with one: we work with L_{rw} .

The three representation matrices we utilise in this paper are thus A, L and L_{rw} .

We use the common nomenclature that the set of eigenvalues of a matrix is called its spectrum. In order to distinguish eigenvalues of A, L and L_{rw} we use μ for an eigenvalue of A , λ for an eigenvalue of L and η for one of L_{rw} . We write $\lambda(\hat{L})$ to denote an eigenvalue of a perturbation \hat{L} of L , and likewise for the other matrices.

A. Motivation of the affine transformations

For d -regular graphs, since $D = dI$, the spectra of the three graph representation matrices are exactly related via known affine transformations, see for example [16, p. 71]. For general graphs, the relation of the representation spectra is non-linear. The transformation between representation spectra can be shown to be either non-existent, if repeated eigenvalues in one spectrum correspond to unequal eigenvalues in another spectrum, or to be polynomial of degree smaller or equal than n , see Appendix A. In practice, finding the polynomial mapping between spectra is subject to significant numerical issues, which are also outlined in Appendix A; furthermore, crucial spectral properties such as eigengap size and eigenvalue ordering are not preserved by these non-linear transformations. Importantly, in the spectral clustering algorithm, eigengaps are used to determine the number of clusters present in the network, while the eigenvalue ordering, an even more fundamental property, is used to identify which eigenvectors to consider [17]. Therefore, when comparing the impact of the choice of the representation matrices on graphical analysis, we need to preserve eigenvalue ordering and eigengap size.

In this paper we consider affine transformations between spectra corresponding to general graphs and bound the resulting eigenvalue differences. Affine transformations preserve eigenvalue ordering and eigengap size. Further details on the properties of the affine transformations are given in Section V.

Comparing the representation spectra without transforming first or only using an additive constant will not yield an informative comparison. This is due to the ordering of eigenvalues being reversed between the adjacency matrix and the Laplacian matrices, i.e., the largest eigenvalue of the adjacency matrix corresponds to the smallest eigenvalue of the Laplacians (see

Section II). Therefore, a reflection of one of the spectra using a multiplicative constant is a sensible preprocessing step before comparing spectra. Furthermore, using an affine transformation has the advantage that we are able to map the spectral supports of the three representation matrices onto each other to further increase comparability of the spectra. This mapping of spectral supports requires scaling.

Let X and Y be any possible pair of the three representation matrices to be compared. Our general approach is to define an affine transform of one of them, say $\mathcal{F}(X)$. We then study bounds on the eigenvalue error

$$|\lambda_i(\mathcal{F}(X)) - \lambda_i(Y)|,$$

where $\lambda_i(Y)$ is the eigenvalue of Y .

Remark 1: For d -regular graphs our transformations recover the exact relations between the spectra of the three matrices. This is a crucial baseline to test when considering maps between the representation spectra. \square

B. Contributions

The contributions of this paper are:

- 1) A framework under which the representation matrices can be compared. Central to this framework is an affine transformation, mapping one matrix as closely as possible on to the other in spectral norm. This procedure is rather general and is likely to be applicable in other matrix comparisons. Properties of these transforms, such as normalised eigengap preservation, are discussed.
- 2) The quantification of the spectral difference between the representation matrices at an individual eigenvalue level, and at eigengap level, via closed form bounds.
- 3) A partition of graphs, according to their degree extremes, derived from the bounds, which enables an interesting analysis of our results.
- 4) The recognition that if the degree extreme difference is large, different choices of representation matrix may give rise to disparate inference drawn from graph signal processing algorithms; smaller degree extreme differences will result in consistent inference, whatever the choice of representation matrix.

In Sections II, III and IV, bounds are provided for the eigenvalue difference between any two of the three representation matrices, A, L and L_{rw} . The properties of the transformation used in each comparison are elaborated in Section V. The analysis of the bound values over all graphs partitioned by their degree extremes is given in Sections VI and VII. Section VIII displays a proof of concept by applying the bounds to graphs arising from a social network and three further model examples, and finds tightness of one of the bounds on two of the examples. In Section IX the bound on normalised eigengap differences for each of the pairs of representation matrices is derived. These bounds are illustrated via examples with varying degree extreme difference in Section X. In Section XI we present the spectral clustering of several graphs to illustrate the effects of the representation matrix choice in practice. Section XII provides a summary and conclusions.

II. BOUNDING THE INDIVIDUAL EIGENVALUE DIFFERENCE FOR A AND L

Let A have eigenvalues $\mu_n \leq \dots \leq \mu_1$. Then, with \iff denoting ‘if and only if,’ for any eigenvalue μ and eigenvector w , we have, for $d_1 \in \mathbb{R}$,

$$\begin{aligned} & Aw = \mu w \\ \iff & (d_1 I - D + D - A)w = (d_1 - \mu)w \\ \iff & (d_1 I - D + L)w = (d_1 - \mu)w \\ \iff & \hat{L}w = \lambda(\hat{L})w, \end{aligned}$$

where

$$\hat{L} \stackrel{\text{def}}{=} d_1 I - D + L = d_1 I - A \quad (2)$$

$$\lambda(\hat{L}) \stackrel{\text{def}}{=} d_1 - \mu. \quad (3)$$

\hat{L} is an affine transform $\mathcal{F}(A)$ of A with transform parameter d_1 . It can also be viewed as a perturbation of L with diagonal ‘error’ $d_1 I - D$, allowing us to find an error bound on the accuracy of the eigenvalue approximation of the unnormalised Laplacian eigenvalues, λ_i , by the eigenvalues of \hat{L} , denoted $\lambda_i(\hat{L})$. In general \hat{L} does not itself have graph Laplacian structure, since, for non- d -regular graphs, not all row sums of \hat{L} are equal to zero, a property of a graph Laplacian. A multiplicative free parameter, in addition to the parameter d_1 , yields no improvement of the final result, and is hence omitted.

In order to relate the eigenvalues of the adjacency matrix A and unnormalised graph Laplacian L , we look at the error in the direct spectral relation via \hat{L} . From (3), we can see that the spectrum in this direct relation gets reordered, i.e., the larger end of the spectrum of the adjacency matrix A corresponds to the smaller end of \hat{L} . Therefore, we will order the eigenvalues of the unnormalised graph Laplacian in opposite order to the ones of the adjacency matrix and denote them by $\lambda_1 \leq \dots \leq \lambda_n$, with corresponding eigenvectors v_1, \dots, v_n .

In order to obtain a bound on the eigenvalue error $|\lambda_i(\hat{L}) - \lambda_i|$, we will utilise the spectral norm $\|\cdot\|_2$. Since A , L and L_{sym} are all real and symmetric, we pay particular attention to real, symmetric matrices, noting again that L_{sym} and L_{rw} have the same eigenvalues.

Definition 1: The spectral norm, or Euclidean 2-norm, of a matrix B , is defined to be the largest singular value of B , i.e. $\|B\|_2 \stackrel{\text{def}}{=} [\max \text{eigenvalue of } (B^T B)]^{1/2}$. For any real, symmetric matrix, singular values and eigenvalues coincide in absolute value. Hence, we can express the spectral norm of a real, symmetric matrix C , with ordered eigenvalues $\lambda_1(C), \dots, \lambda_n(C)$, as $\|C\|_2 = \max(|\lambda_1(C)|, |\lambda_n(C)|)$. \square

Now, we proceed to analyse the error made by approximating λ_i by $\lambda_i(\hat{L})$. Firstly, [1, eqn. (4.3), Chapter 4.1]

$$\|\hat{L} - L\|_2 \geq |\lambda_i(\hat{L}) - \lambda_i| = |d_1 - \mu_i - \lambda_i|, \quad (4)$$

for $i \in \{1, 2, \dots, n\}$, i.e., the difference of the eigenvalues of a symmetric matrix L and its perturbed version \hat{L} is bounded

by the two norm of the perturbation $\hat{L} - L$. Now,

$$\begin{aligned} \|\hat{L} - L\|_2 &\stackrel{(2)}{=} \|d_1 I - D\|_2 \\ &= \max(|d_1 - d_{\max}|, |d_1 - d_{\min}|) \\ &= \frac{d_{\max} - d_{\min}}{2}, \end{aligned} \quad (5)$$

where $d_1 = (d_{\max} + d_{\min})/2$. (5) uses the fact that the eigenvalues of diagonal matrices are equal to their diagonal elements. Furthermore, d_1 is chosen to minimise the upper bound on the approximation error. So, our affine transformation and parameter choice can be conceptualized as

$$A \rightarrow \mathcal{F}_1(A) \stackrel{\text{def}}{=} \hat{L} \approx L,$$

where $\mathcal{F}_1(A)$ is the affine transform specified in (2). Putting (4) and (5) together,

$$|\lambda_i(\hat{L}) - \lambda_i| \leq \frac{d_{\max} - d_{\min}}{2} \stackrel{\text{def}}{=} e(A, L), \quad (6)$$

where we denote the final (error) bound by $e(A, L)$.

Remark 2: The result in (6) can also be obtained from Weyl’s inequality, as shown in Appendix B. \square

For d -regular graphs, (6) gives $e(A, L) = 0$, so that $\lambda_i(\hat{L}) = \lambda_i$ and (3) then gives $\lambda_i = d_1 - \mu_i = d - \mu_i$, i.e., the eigenvalues are related by the required exact relation, as claimed in Remark 1.

For general graphs, using (6), we can establish a rough correspondence, to within an affine transformation, between the eigenvalues of the adjacency matrix, A , and the unnormalised graph Laplacian, L , if the extremes of the degree sequence d_{\max} and d_{\min} are reasonably close.

III. BOUNDING THE INDIVIDUAL EIGENVALUE DIFFERENCE FOR L AND L_{rw}

We now look at the spectral relationship between L and L_{rw} . As in Section II, let L have eigenvalues λ and eigenvectors v . Then, with $c_1 \in \mathbb{R}$,

$$\begin{aligned} Lv &= \lambda v \\ \iff c_1 D D^{-1} L v &= c_1 \lambda v \\ \iff c_1 D L_{rw} v &= c_1 \lambda v \\ \iff \hat{L}_{rw} v &= \eta(\hat{L}_{rw}) v, \end{aligned}$$

where

$$\hat{L}_{rw} \stackrel{\text{def}}{=} c_1 D L_{rw} = c_1 L \quad (7)$$

$$\eta(\hat{L}_{rw}) \stackrel{\text{def}}{=} c_1 \lambda. \quad (8)$$

\hat{L}_{rw} is an affine transform $\mathcal{F}(L)$ of L with transform parameter c_1 . It can also be viewed as a multiplicative perturbation of L_{rw} , via perturbation factor $c_1 D$. Therefore, we also choose a scaling as the eigenvalue transformation and have c_1 as the only free parameter. (Adding a free translation can easily be shown to yield no improvement of the final bound.) The multiplicative transformation between matrices also rules out Weyl’s inequality for finding the bound (see Remark 2).

The following result is the equivalent of (4):

$$\|\hat{L}_{rw} - L_{rw}\|_2 \geq |\eta_i(\hat{L}_{rw}) - \eta_i| = |c_1 \lambda_i - \eta_i|, \quad (9)$$

for $i \in \{1, 2, \dots, n\}$. In the steps that follow we use firstly that the eigenvalues of L_{rw} are all positive, and secondly that $\|L_{rw}\|_2 \leq 2$; as established in [16, p. 64]. Now,

$$\begin{aligned} \left\| \hat{L}_{rw} - L_{rw} \right\|_2 &= \|(c_1 D - I) L_{rw}\|_2 \\ &\leq \|L_{rw}\|_2 \|c_1 D - I\|_2 \\ &\leq 2 \max(|d_{\max} c_1 - 1|, |d_{\min} c_1 - 1|), \quad (10) \\ &= 2 \frac{d_{\max} - d_{\min}}{d_{\max} + d_{\min}}, \end{aligned}$$

where $c_1 \stackrel{\text{def}}{=} 2/(d_{\max} + d_{\min}) = 1/d_1$. The choice for c_1 minimises the upper bound on the error. So in this case the affine transformation and parameter choice have the effect

$$L \rightarrow \mathcal{F}_2(L) \stackrel{\text{def}}{=} \hat{L}_{rw} \approx L_{rw},$$

where $\mathcal{F}_2(L)$ is the affine transform specified in (7). The error bound $e(L, L_{rw})$ satisfies

$$\left| \eta_i(\hat{L}_{rw}) - \eta_i \right| \leq 2 \frac{d_{\max} - d_{\min}}{d_{\max} + d_{\min}} \stackrel{\text{def}}{=} e(L, L_{rw}). \quad (11)$$

Asymptotically, as $d_{\max} \rightarrow \infty$ with fixed $d_{\min} > 0$, the bound tends to 2. The restricted range of d_{\min} is due to D^{-1} , the normalised Laplacian and therefore the bound $e(L, L_{rw})$ not being defined for $d_{\min} = 0$. As in Section II, for d -regular graphs, where $d_{\max} = d_{\min} = d$, the bound equals zero. Hence, the spectra of \hat{L}_{rw} and L_{rw} are equal and from (8), $\eta_i = c_1 \lambda_i = \lambda_i/d$, i.e., the eigenvalues are related by the required exact relation, as claimed in Remark 1.

Overall, the behaviour of this bound is similar to $e(A, L)$ obtained in Section II. The smaller the difference of the degree sequence extremes d_{\max} and d_{\min} , the closer the spectra of L and L_{rw} are related, as signified by a smaller bound on the eigenvalue differences.

IV. BOUNDING THE INDIVIDUAL EIGENVALUE DIFFERENCE FOR A AND L_{rw}

Now we move on to the final of our three possible relations: the spectra of A and L_{rw} . Let L_{rw} have eigenvalues $\eta_1 \leq \dots \leq \eta_n$. Now, with $c_2, d_2 \in \mathbb{R}$,

$$\begin{aligned} Aw &= \mu w \\ \iff (d_2 I - D + L) w &= (d_2 - \mu) w \\ \iff c_2 (d_2 I - D + DL_{rw}) w &= c_2 (d_2 - \mu) w \\ \tilde{L}_{rw} w &= \eta(\tilde{L}_{rw}) w, \quad (12) \end{aligned}$$

where

$$\begin{aligned} \tilde{L}_{rw} &\stackrel{\text{def}}{=} c_2 (d_2 I - D + DL_{rw}) \\ &= c_2 (d_2 I - A) \quad (13) \end{aligned}$$

$$\eta(\tilde{L}_{rw}) \stackrel{\text{def}}{=} c_2 (d_2 - \mu). \quad (14)$$

\tilde{L}_{rw} is an affine transform of A with transform parameters c_2 and d_2 . It can also be viewed as an additive and multiplicative perturbation of L_{rw} . The affine transformation, followed by the parameter choices, will therefore correspond to

$$A \rightarrow \mathcal{F}_3(A) \stackrel{\text{def}}{=} \tilde{L}_{rw} \approx L_{rw},$$

where $\mathcal{F}_3(A)$ is the affine transform specified in (13). Note again that we require $d_{\min} > 0$ due to L_{rw} not being well-defined for $d_{\min} = 0$.

We now have two free parameters, c_2 and d_2 , which will be chosen to minimise the upper bound on the eigenvalue differences. We start with

$$\left\| \tilde{L}_{rw} - L_{rw} \right\|_2 \geq \left| \eta_i(\tilde{L}_{rw}) - \eta_i \right| = |c_2(d_2 - \mu_i) - \eta_i|, \quad (15)$$

for $i \in \{1, 2, \dots, n\}$. Then,

$$\begin{aligned} \left\| \tilde{L}_{rw} - L_{rw} \right\|_2 &= \|c_2 d_2 I - c_2 D + (c_2 D - I) L_{rw}\|_2 \\ &\leq \|c_2 d_2 I - c_2 D\|_2 + 2 \|c_2 D - I\|_2 \quad (16) \\ &\leq |c_2| \frac{d_{\max} - d_{\min}}{2} \\ &\quad + 2 \max(|d_{\max} c_2 - 1|, |d_{\min} c_2 - 1|). \quad (17) \end{aligned}$$

We choose $d_2 = (d_{\max} + d_{\min})/2$ exactly as in (5), since the term being minimized is identical in both cases. The choice of c_2 is involved, since it appears in both terms; details are given in Appendix C, where we see that the choice $c_2 = 2/(d_{\max} + d_{\min})$ means that

$$e(A, L_{rw}) \stackrel{\text{def}}{=} 3 \frac{d_{\max} - d_{\min}}{d_{\max} + d_{\min}}. \quad (18)$$

For d -regular graphs, the bound equals zero and hence the spectra of \tilde{L}_{rw} and L_{rw} are equal and from (14), $\eta_i = c_2(d_2 - \mu_i) = 1 - (\mu_i/d)$, i.e., the spectra of L_{rw} and A are related by the required exact relation.

Remark 3: In Appendix C an alternative bound, $e'(A, L_{rw})$ given in (35), is found. This is tighter, but the corresponding transformation is degenerate. We hence prefer (18), but will also show $e'(A, L_{rw})$ in visualisations in Section VIII. \square

V. NATURE OF TRANSFORMATIONS

In order to motivate the transformations of the spectra further we will visualise them on a real data set and also analyse their properties. We will refer to the transformations in (3), (8) and (14) as f_1, f_2 and f_3 , respectively. Here $d_1 = d_2 = (d_{\max} + d_{\min})/2$ and $c_1 = c_2 = 2/(d_{\max} + d_{\min})$.

$$f_1(\mu) = d_1 - \mu; \quad (19)$$

$$f_2(\lambda) = c_1 \lambda; \quad (20)$$

$$f_3(\mu) = c_2(d_2 - \mu) = 1 - c_2 \mu. \quad (21)$$

A. Karate data example

We first apply the transforms to the spectra of Zachary's karate dataset, which will be further analysed in Section VIII.

The karate dataset was obtained from [2] and dates back to [19]. We work with a square matrix with 34 entries, 'ZACHE,' which is the adjacency matrix of a social network describing presence of interaction in a university karate club. This data set is a common benchmark in the literature, as it lends itself to clustering; see, e.g., [4], [5], [8], [10].

The untransformed and transformed eigenvalues of the representation matrices A, L and L_{rw} of Zachary's karate dataset are shown in Fig. 1. The eigenvalue spectra become more comparable via the proposed transformations. From Figs. 1(d),

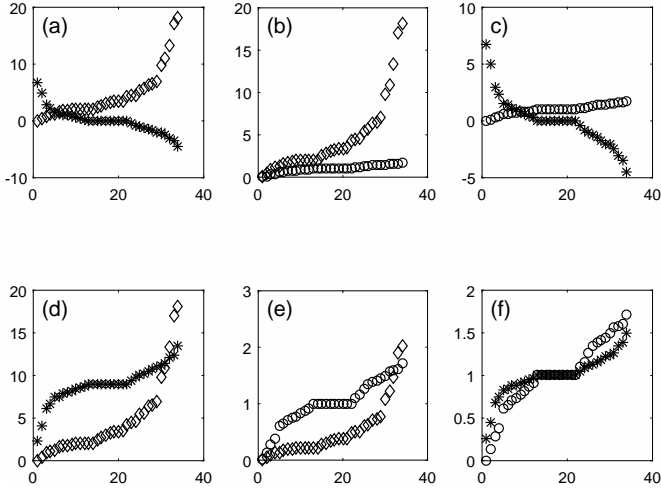


Fig. 1. Results for Zachary's karate dataset. First row: (a) eigenvalues μ of A (stars) and λ of L (diamonds); (b) eigenvalues λ of L and η of L_{rw} (circles); (c) eigenvalues μ of A and η of L_{rw} . Second row: the first of the two eigenvalue spectra are transformed by their respective transformations f_1, f_2 and f_3 .

(e) and (f) it can be observed that each pair of spectra of the karate dataset cover a similar range after transformation. However, they don't coincide and it can be argued that they carry different information about the underlying network.

B. Transformation properties

All three transformations f_1, f_2 and f_3 are affine. The following simple observations are made for general affine transformations $g(x) = ax + b$, where $a, b \in \mathbb{R}, a \neq 0$.

1) *Ordering*: Ordering is preserved:

$$\begin{aligned} \mu_1 &\geq \mu_2 \\ \iff a\mu_1 + b &\geq a\mu_2 + b \\ \iff g(\mu_1) &\geq g(\mu_2). \end{aligned}$$

2) *Eigengaps*: Next we show that eigengaps, relative to the spectral support, are preserved. Assume that the domain of g is equal to the interval $[x_1, x_2]$. Hence g 's image is equal to $[g(x_1), g(x_2)]$. Then normalised eigengaps are preserved:

$$\frac{\mu_1 - \mu_2}{x_2 - x_1} = \frac{a(\mu_1 - \mu_2) + b - b}{a(x_2 - x_1) + b - b} = \frac{g(\mu_1) - g(\mu_2)}{g(x_2) - g(x_1)}. \quad (22)$$

3) *Mapping of spectral supports*: As a final property we show the mappings for the spectral supports of the different representation matrices. The spectral supports of the three representation matrices can be derived via Gershgorin's theorem and are given in [16, p. 29, p. 64, p. 68].

$$f_1 : [-d_{\max}, d_{\max}] \rightarrow \left[-\frac{d_{\max} - d_{\min}}{2}, \frac{3d_{\max} + d_{\min}}{2} \right] \quad (23)$$

$$f_2 : [0, 2d_{\max}] \rightarrow \left[0, \frac{4d_{\max}}{d_{\max} + d_{\min}} \right] \quad (24)$$

$$f_3 : [-d_{\max}, d_{\max}] \rightarrow \left[-\frac{d_{\max} - d_{\min}}{d_{\max} + d_{\min}}, \frac{3d_{\max} + d_{\min}}{d_{\max} + d_{\min}} \right]. \quad (25)$$

Remark 4: It is possible to choose the transformation parameters so that the transformation maps exactly to the spectral support of the target matrix. However, this results in a greater bound on the eigenvalue differences. Rather, since the mapped supports are of little consequence, we choose our transformation parameters according to the bound value, their treatment of eigenvalue ordering, and relative eigengap preservation. \square

VI. RELATING THE SPECTRAL BOUNDS

We now compare the spectral bounds with each other and illustrate their relationship. Firstly,

$$\begin{aligned} e(A, L) &\leq e(L, L_{rw}) \\ \iff \frac{d_{\max} - d_{\min}}{2} &\leq 2 \frac{d_{\max} - d_{\min}}{d_{\max} + d_{\min}} \\ \iff d_{\max} + d_{\min} &\leq 4. \end{aligned} \quad (26)$$

Next,

$$\begin{aligned} e(A, L) &\leq e(A, L_{rw}) \\ \iff \frac{d_{\max} - d_{\min}}{2} &\leq 3 \frac{d_{\max} - d_{\min}}{d_{\max} + d_{\min}} \\ \iff d_{\max} + d_{\min} &\leq 6. \end{aligned} \quad (27)$$

Finally,

$$\begin{aligned} e(L, L_{rw}) &\leq e(A, L_{rw}) \\ \iff 2 \frac{d_{\max} - d_{\min}}{d_{\max} + d_{\min}} &\leq 3 \frac{d_{\max} - d_{\min}}{d_{\max} + d_{\min}}, \end{aligned} \quad (28)$$

which, obviously, always holds.

For easier analysis of these inequalities, we display some sample values in Table I. The first column of Table I only contains values of $e(A, L)$ as for $d_{\min} = 0$ the normalised Laplacian and hence $e(L, L_{rw})$ and $e(A, L_{rw})$ are not well-defined. In practice this is of little consequence since disconnected nodes are commonly removed from the dataset as a preprocessing step.

In Table I the bound values are separated into 6 different regions. We start off with the diagonal from which it is clear that, when $d_{\max} = d_{\min}$, i.e., for d -regular graphs, we have a direct spectral relation.

For the $d_{\max} + d_{\min} < 4$ region (**bold**), we find that $e(A, L)$ is the smallest of the three bounds, and the spectra of A and L are the most closely related. We were able to anticipate this result via (26) and (27).

Now for $d_{\max} + d_{\min} = 4$ (underlined), we find that $e(A, L) = e(L, L_{rw})$, while $e(A, L_{rw})$ is still larger than the other two.

From inequalities (26) and (27), we expect that the ordering of the bound values changes for $d_{\max} + d_{\min} = 5$ (teletype). The values show us that the spectra of A and L_{rw} are now furthest apart. As expected, the spectra of L and L_{rw} have the closest relation, i.e., the smallest bound value on their eigenvalue differences. $e(L, L_{rw})$ will remain the smallest bound of the three for all $d_{\max} + d_{\min} \geq 5$.

When $d_{\max} + d_{\min} = 6$ (*italic*), we have another transition point, where $e(A, L) = e(A, L_{rw})$.

		d_{\min}					
		0	1	2	3	4	5
d_{\max}	1	(0.5, ·, ·)	(0, 0, 0)	*	*	*	*
	2	(1, ·, ·)	(0.5, 0.67, 1)	(0, 0, 0)	*	*	*
	3	(1.5, ·, ·)	<u>(1, 1, 1.5)</u>	(0.5, 0.4, 0.6)	(0, 0, 0)	*	*
	4	<u>(2, ·, ·)</u>	(1.5, 1.2, 1.8)	(1, 0.67, 1)	(0.5, 0.29, 0.43)	(0, 0, 0)	*
	5	(2.5, ·, ·)	(2, 1.33, 2)	(1.5, 0.86, 1.29)	(1, 0.5, 0.75)	(0.5, 0.22, 0.33)	(0, 0, 0)
	6	(3, ·, ·)	(2.5, 1.43, 2.14)	(2, 1, 1.5)	(1.5, 0.67, 1)	(1, 0.4, 0.6)	(0.5, 0.18, 0.27)
	7	(3.5, ·, ·)	(3, 1.5, 2.25)	(2.5, 1.11, 1.67)	(2, 0.8, 1.2)	(1.5, 0.55, 0.82)	(1, 0.33, 0.5)

TABLE I

COMPARING BOUNDS ON EIGENVALUE DIFFERENCES OF A , L AND L_{rw} . THE BOUND VALUES ARE DISPLAYED AS $(e(A, L), e(L, L_{rw}), e(A, L_{rw}))$. THE 6 DIFFERENT REGIONS ARE LABELLED AS FOLLOWS: $e(A, L) = e(L, L_{rw}) = e(A, L_{rw}) = 0$ AS **BOLD AND UNDERLINED**, $e(A, L) < e(L, L_{rw}) < e(A, L_{rw})$ AS **BOLD**, $e(A, L) = e(L, L_{rw}) < e(A, L_{rw})$ AS UNDERLINED, $e(L, L_{rw}) < e(A, L) < e(A, L_{rw})$ AS TELETYPE, $e(L, L_{rw}) < e(A, L) = e(A, L_{rw})$ AS *italic* AND FINALLY $e(L, L_{rw}) < e(A, L_{rw}) < e(A, L)$ IN NORMAL FONT.

Finally, with $d_{\max} + d_{\min} > 6$ (normal font), we enter the last region, which will apply to the majority of graphs. Here the spectra of L and L_{rw} have the closest relation, while the bound on the eigenvalue difference of A and L is the largest. It is interesting to note, that since the spectral support of neither A , nor L , is bounded, the bound on their eigenvalue difference is also not bounded above. This does not apply to the other two bounds as we have $e(L, L_{rw}) \leq 2$ and $e(A, L_{rw}) \leq 3$.

VII. EXPLAINING THE STRUCTURE OF TABLE I

We begin the forthcoming analysis with the definition of connected components in a graph.

Definition 2: A path on a graph G is an ordered list of unique vertices such that consecutive vertices are connected by an edge. A vertex set S_k is called a *connected component* if there exists a path between any two vertices $v_i, v_j \in S_k$ and there exists no path from any $v_i \in S_k$ to any $v_j \notin S_k$. \square

A. Partitioning

We will illustrate the class of unweighted graphs characterised by certain degree extremes d_{\min} and d_{\max} in order to visualise the class of graphs to which the bounds apply. This will allow us to explain the monotonicity of the three bounds in the sense of Table I. We will denote the class of graphs with $d_{\min} = j$ and $d_{\max} = k$ by $\mathcal{C}_{j,k}$. For any graph, d_{\min} and d_{\max} are unique, and hence no graph is in two or more classes of $\{\mathcal{C}_{j,k}\}_{j=0}^k$. Therefore, the classes $\{\mathcal{C}_{j,k}\}_{j=0}^k$ are disjoint. Furthermore, since the degree extremes of a graph always exist, we have that $\{\mathcal{C}_{j,k}\}_{j=0}^k$ is a partition of the class of graphs with $d_{\max} = k$, (denoted by $\mathcal{C}_{\cdot,k}$ in the following).

For illustrative purposes, we consider the class of graphs $\mathcal{C}_{\cdot,2}$, i.e., the class of graphs to which the bounds in the second row of Table I apply. In Fig. 2 we display the partition of $\mathcal{C}_{\cdot,2}$, with examples of elements in each class. All classes $\mathcal{C}_{j,k}$ are infinite in size, so only a few arbitrary sample elements are displayed here. The elements of each class are marked by dashed ellipses. Graph G_3 is an element of $\mathcal{C}_{0,2}$ and consists of five connected components. Graphs in $\mathcal{C}_{0,2}$ are denoted by G_a , graphs in $\mathcal{C}_{1,2}$ by H_a and graphs in $\mathcal{C}_{2,2}$ by I_a for $a \in \mathbb{Z}$.

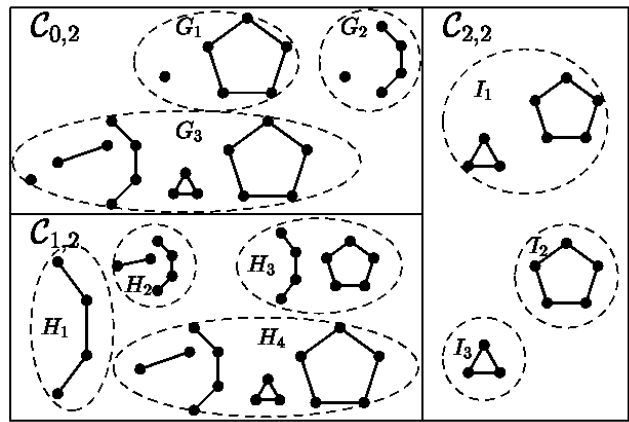


Fig. 2. This figure illustrates the partition $\mathcal{C}_{\cdot,2} = \mathcal{C}_{0,2} \cup \mathcal{C}_{1,2} \cup \mathcal{C}_{2,2}$. Examples of elements of the classes $\mathcal{C}_{0,2}$ containing all graphs with $d_{\min} = 0$ and $d_{\max} = 2$, $\mathcal{C}_{1,2}$, with element for which $d_{\min} = 1$ and $d_{\max} = 2$ and $\mathcal{C}_{2,2}$, the class of 2-regular graphs are shown.

B. Adding and deleting connected components

We now turn to a specific manipulation of graphs — addition and removal of connected components — which allows us to order the spectra of the graphs and hence understand the monotonicity observed in the bounds in rows of Table I.

In Fig. 2, we see that we can obtain G_3 from H_4 by adding a single disconnected vertex and that we can obtain H_4 from I_1 by adding the connected components, the line and the 2-complete component. In general, we can obtain a graph in $\mathcal{C}_{j,k}$ from a graph in $\mathcal{C}_{j+1,k}$, for all $j \leq k - 1, k \in \mathbb{N}$, by adding to the graph one or more connected components in which all vertices are of degree greater or equal to j and smaller or equal to k , with at least one vertex attaining degree j .

C. Analysis of bound monotonicity in rows of Table I

As stated in [6, p. 7], the spectrum of a graph is the union of the spectra of its connected components, i.e., the union of the sets of eigenvalues of the representation matrices corresponding to the connected components. Since all graphs in $\mathcal{C}_{j,k}$ can be obtained from graphs in $\mathcal{C}_{j+1,k}$ by adding one or more connected components, it can be argued that all spectra of graphs in $\mathcal{C}_{j+1,k}$ are subsets of spectra of graphs

in $\mathcal{C}_{j,k}$. Therefore, the support of the spectra of graphs in $\mathcal{C}_{j,k}$ must be larger or equal to the support of spectra of graphs in $\mathcal{C}_{j+1,k}$. Hence, we expect the spectral bounds we derived to be decreasing or constant with increasing d_{\min} and constant d_{\max} . This phenomenon can be observed in Table I when traversing each row.

D. Analysis of bound monotonicity in columns of Table I

In Section VII-B, when traversing the rows of Table I, we were adding connected components to graphs in $\mathcal{C}_{j+1,k}$ to obtain graphs in $\mathcal{C}_{j,k}$. We observed decreasing bound size with increasing indices corresponding to d_{\min} . Here we find increasing bound size with increasing indices corresponding to d_{\max} : it seems sensible that increasing the support of the degree distribution should also increase the spectral support and hence the bounds. (The *degree distribution* is a probability distribution from which vertex degrees of a graph are sampled.)

We argue that any graph in $\mathcal{C}_{j,k+1}$, can be obtained from a graph in $\mathcal{C}_{j,k}$, by adding a connected component with all vertex degrees greater or equal to j and smaller or equal than $k+1$ with at least one node attaining degree $k+1$. Then the argument goes exactly as in Section VII-C, that spectra of graphs in $\mathcal{C}_{j,k}$ are subsets of spectra of graphs $\mathcal{C}_{j,k+1}$ and therefore the spectral support and hence the spectral bounds on $\mathcal{C}_{j,k+1}$ have to be greater or equal than the respective quantities for $\mathcal{C}_{j,k}$. Again, this kind of monotonicity is observed when comparing bound values in the *columns* of Table I.

VIII. VISUALISING THE EIGENVALUE BOUNDS ON DATA

In this section we illustrate the bounds on the spectra of Zachary's karate dataset, which we already met in Section V-A. We then proceed to explore the bounds on three different graphs with $d_{\min} = 1$ and $d_{\max} = 17$, choices appropriate for the karate dataset.

The graph defined in the karate data set is plotted in Fig. 3(a) together with the three graph examples in Figs. 3(b)-(d) analysed in Section VIII-B.

A. Zachary's karate dataset

In Fig. 4, we display a proof of concept of the bounds derived in this document. We display the transformed eigenvalues together with the eigenvalues we compare to and the derived bounds. The eigenvalue bounds are centred around the average value of each eigenvalue pair in order to highlight the maximal difference achievable by each individual eigenvalue pair under comparison. For the karate dataset the bound values $(e(A, L), e(L, L_{rw}), e(A, L_{rw}))$ are equal to $(8.00, 1.78, 2.67)$. With $d_{\min} = 1$ and $d_{\max} = 17$ these bounds clearly fall into the region characterised last in Section VI, for which $d_{\max} + d_{\min} > 6$. The values in plot (a) are much larger than the ones in plots (b) and (c), as was to be expected from the analysis in Section VI. The particular bounds displayed here are valid for all graphs with $d_{\min} = 1$ and $d_{\max} = 17$, i.e., all graphs in $\mathcal{C}_{1,17}$. The fact of the bounds being almost attained in plot (a), and not attained in plot (c), is more a

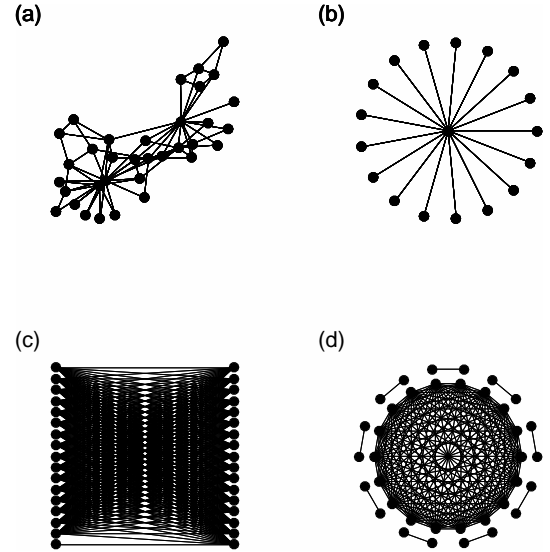


Fig. 3. (a) graph given by the karate data set. (b) graph A, the star graph on 18 nodes. (c) graph B, a bipartite graph with degree distribution $\{1, \{16\}^{16}, \{17\}^{17}\}$ (see Section VIII-B). (d) graph C, a graph consisting of 9 2-complete components and one 18-complete component.

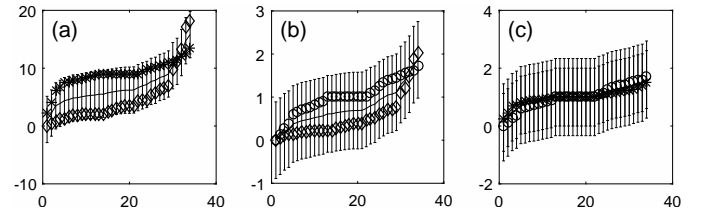


Fig. 4. Eigenvalue bounds on the karate eigenvalues. In plot (a) we display the bound $e(A, L)$ via the intervals together with the transformed eigenvalues of the adjacency matrix $f_1(\mu)$ (stars) and the eigenvalues of the Laplacian λ (diamonds). (b) the bound $e(L, L_{rw})$ is displayed via the intervals, the diamonds correspond to the transformed Laplacian eigenvalues $f_2(\lambda)$ and the circles are the eigenvalues of the normalised graph Laplacian η . In plot (c) the inner bounds interval corresponds to $e'(A, L_{rw})$, (see Remark 3), while the outer interval corresponds to the bound $e(A, L_{rw})$, the stars correspond to the transformed adjacency eigenvalues $f_3(\mu)$ and the circles are the normalised Laplacian eigenvalues η .

consequence of the structure of the graph given by the karate data set than tightness and quality of the bounds. Since the three bounds $e(A, L)$, $e(L, L_{rw})$ and $e(A, L_{rw})$ apply to entire classes $\mathcal{C}_{j,k}$ at a time, we can only hope to achieve tightness on these classes (hence the bounds being attained for some elements in $\mathcal{C}_{j,k}$), and not on each individual element of them.

B. Three examples exploring the bounds for graphs in $\mathcal{C}_{1,17}$

We now proceed to explore the class of graphs with $d_{\min} = 1$ and $d_{\max} = 17$, $\mathcal{C}_{1,17}$, to which the bounds for the karate dataset displayed in Fig. 4 apply. We will consider the star on 18 vertices, “graph A,” a bipartite graph, “graph B,” and a graph containing several 1- and 17-regular connected components, “graph C.”

1) *Graph A (Star graph)*: Fig. 5 displays the three bounds on the spectra of the star graph with degree sequence $\{\{1\}^{17}, 17\}$, where the notation $\{x\}^y$ is shorthand for the multiset consisting of y elements equal to x .

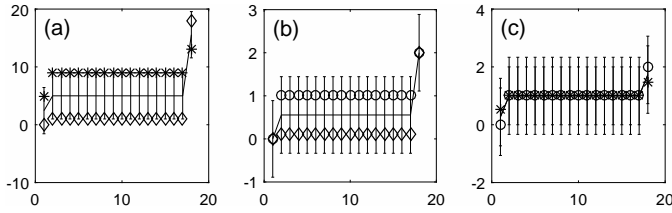


Fig. 5. Spectra and transformed spectra with their bound for graph A, a star on 18 nodes, with degree sequence $\{\{1\}^{17}, 17\}$. The format follows Fig. 4.

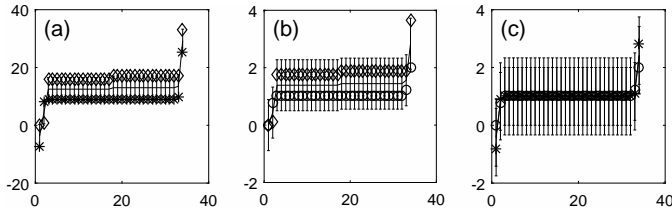


Fig. 6. Spectra and transformed spectra with their bound for graph B, the bipartite graph on 34 nodes, with degree sequence $\{1, \{16\}^{16}, \{17\}^{17}\}$. The format follows Fig. 4.

Especially notable, is that from Fig. 5(a) the bound $e(A, L)$ can be seen to be tight: the spectra of A and L have maximal distance on individual eigenvalue level for 16 of the 18 eigenvalues. Further, for the 16 eigenvalues of maximal distance between spectra of A and L , the spectra of A and L_{rw} coincide, up to transformation.

2) *Graph B (Bipartite graph)*: We will now work with a bipartite graph on 34 nodes. The degree sequence of the bipartite graph is $\{1, \{16\}^{16}, \{17\}^{17}\}$. The graphs falling under the same spectral bound are only restricted in their degree sequence extremes, not by the number of nodes in the graphs.

In Fig. 6(a), 15 of the eigenvalue pairs attain the maximal distance given by the bound and the remaining 19 eigenvalue pairs are close to attaining the maximal distance. Also, all but one of the eigenvalues of the graph Laplacian L are larger than the ones of the adjacency matrix A . Fig. 5 displayed the opposite phenomenon, the eigenvalues of A being mostly larger than the eigenvalues of L . Another, very interesting, phenomenon can be spotted in the behaviour of the first two eigenvalues of A and L in Fig. 6(a). To discuss this we need the following:

Definition 3: Let X and Y be real symmetric matrices with eigenvalues $\lambda_1(X), \dots, \lambda_n(X)$ and $\lambda_1(Y), \dots, \lambda_n(Y)$, respectively and let ϕ be an affine transformation applied to a matrix spectrum. Then, in the context of a bound of the form $h(X, Y) \geq |\phi(\lambda_i(X)) - \lambda_i(Y)|$, we will use the term *maximal crossover* of eigenvalues to express that $\phi(\lambda_i(X))$ attains one of the ends of the bound $h(X, Y)$, $\phi(\lambda_{i+1}(X))$ attains the opposite end of the bound $h(X, Y)$, and vice versa for $\lambda_i(Y)$ and $\lambda_{i+1}(Y)$. \square

We see that the first two eigenvalues of A and L are very close to a maximal crossover, where $\phi = f_1$, with rounded distances $\lambda_1 - f_1(\mu_1) = 7.49$ and $\lambda_2 - f_1(\mu_2) = -7.06$ for a bound value $e(A, L) = 8$. The concept of a maximal crossover

will be significant in Section IX when bounding eigengaps.

Fig. 6(b) also provides an interesting insight: the last two eigenvalues $f_2(\lambda_{34})$ and η_{34} attain the opposing ends of the bound $e(L, L_{rw})$, with a rounded distance between them equal to $f_2(\lambda_{34}) - \eta_{34} = 1.67$ on the bound value $e(L, L_{rw}) = 1.78$. Hence, $e(L, L_{rw})$ is somewhat close to tight on $\mathcal{C}_{1,17}$.

Finally, we see in Fig. 6(c) that the eigenvalues of A and L_{rw} mostly coincide up to transformation, as was the case for the eigenvalues in Fig. 5(c). However, as mentioned previously, this has no particular implication for the tightness of the bound, as the bound applies to a very large class of graphs.

In both Figs. 5 and 6, the difference between the transformed spectrum of the adjacency matrix and the spectrum of the normalised Laplacian is notably smaller than the differences in the other two spectral comparisons. A possible explanation of this phenomenon follows from noticing that the difference between the adjacency matrix A and the normalised Laplacian $L_{rw} = I - D^{-1}A$ is the degree normalisation. It is hence conceivable, that for degree sequences with low ‘variance,’ this normalisation is less impactful and hence we expect a small difference in the spectra. This ‘low variance’ argument is a possible explanation for the small differences observed in Figs. 5(c) and 6(c). This phenomenon positively supports our transformations, specifically f_3 , through recovery of the small difference between the two spectra.

3) *Graph C*: We can easily construct an example for which the spectra $f_3(\mu)$ and η show larger differences by noticing that the value c_2 in the transformation function f_3 is fixed to be equal to $1/9$ for all graphs in $\mathcal{C}_{1,17}$. As we saw in Section VI, $\mathcal{C}_{1,17}$ also contains graphs which consist of several connected components. We hence consider the graph consisting of 9 pairs of vertices connected only to one another, hence 18 nodes of degree 1, and a complete connected component on 18 nodes.

Consider Fig. 7(c): for just the 1-regular components, choosing the scaling to be equal to $c_2^{(1)} = 1$ would yield perfect correspondence of the spectrum of the transformed adjacency matrix and the spectrum of the normalised graph Laplacian (L_{rw}). For just the 17-regular component, the normalisation by $c_2^{(2)} = 1/17$ is ideal. The choice of $c_2 = 1/9$ yields a difference in the transformed spectrum and the untransformed spectrum, since it represents a departure from the case of exact correspondence of spectra. There is a larger difference between the eigenvalues corresponding to the complete graphs on two nodes, since the departure of the scaling factor c_2 from the optimal scaling factor $c_2^{(1)}$ is larger than for the eigenvalues corresponding to the 17-regular component. Correspondence of eigenvalues to different connected components of the graph could be established by observing connected components *separately*, in conjunction with the result in [6] discussed in Section VII-C.

Finally, in Fig. 7(a), we spot a maximal crossover with $\phi = f_1$ between eigenvalues $f_1(\mu_1)$, λ_1 and $f_1(\mu_2)$, λ_2 and again for the pairs with indices 19 and 20.

Remark 5: In the case of a graph consisting of more than one connected component, as in Fig. 7, it is beneficial to consider connected components separately. When this is done, the degree sequence extremes are decreased or stay equal and hence the transformation becomes more accurate

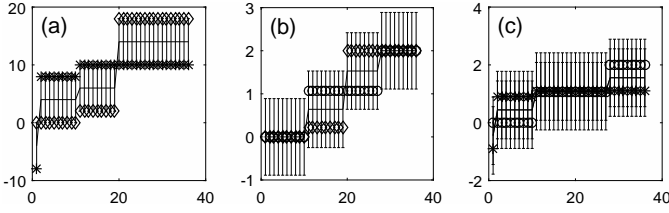


Fig. 7. Spectra and transformed spectra together with their bound for graph C, consisting of 10 connected components, 9 of which are the complete graph on 2 nodes and one of which is the complete graph on 18 nodes. Therefore the degree sequence is equal to $\{\{1\}^{18}, \{17\}^{18}\}$. The format follows Fig. 4.

or stays the same and the bounds decrease or stay equal (see Sections VII-C and VII-D). For graph C underlying Fig. 7, the spectra of the connected components can individually be exactly related as the connected components are 1- and 17-regular. \square

IX. BOUNDS ON NORMALISED EIGENGAP DIFFERENCES

Here we examine the eigengaps corresponding to the three representation matrices. We will compare bounds on eigengaps normalised by the spectral support, to bounds on eigengaps derived from eigenvalues transformed by f_1, f_2 and f_3 . Furthermore, we investigate under which conditions on the spectra the derived eigengap bounds are tight.

A. Normalised eigengap difference of A and L

Let \mathcal{M}_i denote the i^{th} eigengap of A , $\mathcal{M}_i = \mu_i - \mu_{i+1}$ and \mathcal{L}_i denote the i^{th} eigengap of L , $\mathcal{L}_i = \lambda_{i+1} - \lambda_i$ for $i \in \{1, 2, \dots, n-1\}$. Also recall that the spectral support of A and L is equal to $[-d_{\max}, d_{\max}]$ and $[0, 2d_{\max}]$, respectively, so the length of the support is $\ell(\mu) = \ell(\lambda) = 2d_{\max}$.

From (19) and (23),

$$\begin{aligned} \left| \frac{f_1(\mu_{i+1}) - f_1(\mu_i)}{\ell(f_1(\mu))} - \frac{\mathcal{L}_i}{\ell(\lambda)} \right| &= \left| \frac{\mathcal{M}_i}{2d_{\max}} - \frac{\mathcal{L}_i}{2d_{\max}} \right| \\ &= \left| \frac{\mathcal{M}_i}{\ell(\mu)} - \frac{\mathcal{L}_i}{\ell(\lambda)} \right|, \end{aligned}$$

which would be anticipated from (22). Furthermore, $\ell(\mu) = \ell(\lambda)$, so the normalisation of the two bounds separately is equivalent to normalising the entire difference by a single value. This will not be the case in Sections IX-B and IX-C, where the lengths of the eigenvalue supports are different.

The bound on the normalised eigengap difference, denoted

$g(A, L)$, then takes the following form:

$$\begin{aligned} \left| \frac{\mathcal{M}_i}{2d_{\max}} - \frac{\mathcal{L}_i}{2d_{\max}} \right| &= \frac{1}{2d_{\max}} |\mu_i - \mu_{i+1} - \lambda_{i+1} + \lambda_i| \\ &= \frac{1}{2d_{\max}} \left| \mu_i - \frac{d_{\max} + d_{\min}}{2} \right. \\ &\quad \left. + \lambda_i - \mu_{i+1} + \frac{d_{\max} + d_{\min}}{2} - \lambda_{i+1} \right| \\ &= \frac{1}{2d_{\max}} [|\lambda_i - f_1(\mu_i)| \\ &\quad + |f_1(\mu_{i+1}) - \lambda_{i+1}|] \quad (29) \\ &\leq \frac{1}{2d_{\max}} 2e(A, L) \quad (30) \\ &= \frac{d_{\max} - d_{\min}}{2d_{\max}} \stackrel{\text{def}}{=} g(A, L). \end{aligned}$$

The triangle inequality has been used to go from (29) to (30).

It follows from Equation (29), that the bound on the eigengaps is tight if and only if the individual mapped eigenvalue differences $\lambda_i - f_1(\mu_i)$ and $\lambda_{i+1} - f_1(\mu_{i+1})$ have opposing signs and occupy the extremes of the bound $e(A, L)$. In Definition 3, such a situation was called a maximal crossover for general transformations ϕ . We observed in Section VIII, Fig. 6(a), a situation very close to a maximal crossover with $\phi = f_1$. A maximal crossover is shown in Fig. 7(a) for $\phi = f_1$; therefore, $g(A, L)$ is the optimal *constant* bound since it is tight for some cases in $\mathcal{C}_{1,17}$.

B. Normalised eigengap difference of L and L_{rw}

We proceed to derive a bound on the normalised eigengap difference of L and L_{rw} , denoted $g(L, L_{rw})$. Let $\mathcal{N}_i = \eta_{i+1} - \eta_i$ denote the i^{th} eigengap of L_{rw} for $i \in \{1, \dots, n-1\}$. For L_{rw} we recall that $\ell(\eta_i) = 2$.

Firstly, when normalising the transformed eigenvalues by their support, we end up with the comparison of normalised untransformed spectra as proven in Section V, i.e., from (20) and (24),

$$\begin{aligned} \left| \frac{f_2(\lambda_{i+1}) - f_2(\lambda_i)}{\ell(f_2(\lambda))} - \frac{\mathcal{N}_i}{\ell(\eta)} \right| &= \left| \frac{c_1}{\frac{2}{d_{\max} + d_{\min}}} \frac{[\lambda_{i+1} - \lambda_i]}{2d_{\max}} - \frac{\mathcal{N}_i}{2} \right| \\ &= \left| \frac{\mathcal{L}_i}{\ell(\lambda)} - \frac{\mathcal{N}_i}{\ell(\eta)} \right|, \end{aligned}$$

as expected from (22). Now the normalised eigengap difference follows:

$$\begin{aligned} \left| \frac{\mathcal{L}_i}{2d_{\max}} - \frac{\mathcal{N}_i}{2} \right| &= \frac{1}{2} \left| \frac{1}{d_{\max}} (\lambda_{i+1} - \lambda_i) + \eta_i - \eta_{i+1} \right| \quad (31) \\ &\leq \frac{1}{2} \left[\left| \frac{1}{d_{\max}} \lambda_{i+1} - \eta_{i+1} \right| + \left| \frac{1}{d_{\max}} \lambda_i - \eta_i \right| \right], \end{aligned}$$

from the triangle inequality. A comparison with (9), shows that these eigenvalue differences can be bounded by replacing c_1 in (9) by $1/d_{\max}$ and then making this substitution into (10):

$$\begin{aligned}
\left| \frac{\mathcal{L}_i}{2d_{\max}} - \frac{\mathcal{N}_i}{2} \right| &\leq \frac{1}{2} \left[4 \max \left(0, \left| \frac{d_{\min}}{d_{\max}} - 1 \right| \right) \right] \\
&= 2 \left(1 - \frac{d_{\min}}{d_{\max}} \right) \\
&= 2 \frac{d_{\max} - d_{\min}}{d_{\max}} \stackrel{\text{def}}{=} g(L, L_{rw}).
\end{aligned}$$

We see from (31), that observing a maximal crossover with $\phi(\lambda) = \lambda/d_{\max}$ in the normalised spectra, would render $g(L, L_{rw})$ a tight bound.

Remark 6: Suppose we ignore the fact that the spectral support of the eigenvalues is not equal and just compare transformed eigengaps $f_2(\lambda_{i+1}) - f_2(\lambda_i)$ to the eigengaps of L_{rw} . (We still normalise by $1/\ell(\eta) = 1/2$ to have the spectrum of the normalised graph Laplacian have the same support, as in (31).) Then we have

$$\begin{aligned}
\frac{1}{\ell(\eta)} |f_2(\lambda_{i+1}) - f_2(\lambda_i) - \mathcal{N}_i| \\
\leq \frac{1}{2} [|f_2(\lambda_{i+1}) - \eta_{i+1}| + |f_2(\lambda_i) - \eta_i|] \\
\leq e(L, L_{rw}) = 2 \frac{d_{\max} - d_{\min}}{d_{\max} + d_{\min}} \stackrel{\text{def}}{=} g'(L, L_{rw}).
\end{aligned}$$

So, by relaxing the restriction that the eigenvalues should be compared on the same scale, and by normalising by $1/2$, we obtained a smaller bound on the transformed, but unnormalised, eigengaps, i.e., $g'(L, L_{rw}) \leq g(L, L_{rw})$. However, when obtaining $g'(L, L_{rw})$, we compare transformed eigenvalues $f_2(\lambda)/2 \in [0, 2d_{\max}/(d_{\max} + d_{\min})]$ to eigenvalues $\eta/2 \in [0, 1]$. This can be argued to be less intuitive from a practitioners point of view and less well motivated in application. We hence recommend the comparison of eigengaps normalised by the eigenvalue's spectral support and the bound $g(L, L_{rw})$ which results from this comparison. \square

C. Normalised eigengap difference of A and L_{rw}

Finally, we will derive the bound on the normalised eigengaps of A and L_{rw} , denoted by $g(A, L_{rw})$. From (21) and (25), we can see that (22) holds:

$$\begin{aligned}
\left| \frac{f_3(\mu_{i+1}) - f_3(\mu_i)}{\ell(f_3(\mu))} - \frac{\mathcal{N}_i}{\ell(\eta)} \right| &= \left| \frac{c_2}{\frac{2}{d_{\max} + d_{\min}}} \frac{\mu_i - \mu_{i+1}}{2d_{\max}} - \frac{\mathcal{N}_i}{2} \right| \\
&= \left| \frac{\mathcal{M}_i}{\ell(\mu)} - \frac{\mathcal{N}_i}{\ell(\eta)} \right|.
\end{aligned}$$

We hence proceed to find the bound on the normalised eigengaps.

$$\begin{aligned}
\left| \frac{\mathcal{M}_i}{2d_{\max}} - \frac{\mathcal{N}_i}{2} \right| &= \frac{1}{2} \left| \frac{1}{d_{\max}} (\mu_i - \mu_{i+1} + d_2 - d_2) + \eta_i - \eta_{i+1} \right| \\
&\leq \frac{1}{2} \left[\left| \frac{1}{d_{\max}} (d_2 - \mu_{i+1}) - \eta_{i+1} \right| \right. \\
&\quad \left. + \left| \frac{1}{d_{\max}} (d_2 - \mu_i) - \eta_i \right| \right],
\end{aligned}$$

via the triangle inequality. Since the optimisation of d_2 is independent of the scaling factor in (16), we find again that

$d_2 = (d_{\max} + d_{\min})/2$ minimises the bound. Then, a comparison with (15), shows that these eigenvalue differences can be bounded by replacing c_2 by $1/d_{\max}$ and then substituting into (17) to give

$$\begin{aligned}
\left| \frac{\mathcal{M}_i}{2d_{\max}} - \frac{\mathcal{N}_i}{2} \right| &\leq \frac{d_{\max} - d_{\min}}{2d_{\max}} + 2 \max \left(0, \left| \frac{d_{\min}}{d_{\max}} - 1 \right| \right) \\
&= \frac{5}{2} \frac{(d_{\max} - d_{\min})}{d_{\max}} \stackrel{\text{def}}{=} g(A, L_{rw}).
\end{aligned}$$

Again, as in Sections IX-A and IX-B, a maximal crossover with $\phi(\mu) = (d_2 - \mu)/d_{\max}$ in the normalised spectra corresponds to $g(A, L_{rw})$ being a tight bound.

Remark 7: Suppose, as in Section IX-B, we relax the normalisation restriction that both spectra have to be on the same scale after normalisation and compare the transformed eigenvalue gaps to the eigengaps of L_{rw} both normalised by $1/2$:

$$\begin{aligned}
\frac{1}{2} |f_3(\mu_{i+1}) - f_3\mu_i - \mathcal{N}_i| &\leq \frac{1}{2} [|f_3(\mu_{i+1}) - \eta_{i+1}| \\
&\quad + |f_3(\mu_i) - \eta_i|] \\
&\leq e'(A, L_{rw}) \stackrel{\text{def}}{=} g'(L, L_{rw}) \\
&= \begin{cases} 3 \frac{d_{\max} - d_{\min}}{d_{\max} + d_{\min}}, & d_{\max} \leq 5d_{\min}; \\ 2, & \text{otherwise.} \end{cases}
\end{aligned}$$

Although $g'(A, L_{rw}) \leq g(A, L_{rw})$, as in Section IX-B, we advise against $g'(A, L_{rw})$ and in favour of $g(A, L_{rw})$. From a practitioners point of view it is more sensible to compare eigengaps on equal support. \square

X. EIGENGAP BOUND EXAMPLES FOR VARYING DEGREE EXTREMES

In this section we observe our eigengap bounds on examples with varying degree extremes. The functional form of our bounds implies that a growing degree extreme difference allows for a greater spectral difference between graph representation matrices. We visualise this effect by varying the degree maximum in graph C by replacing the 18-complete component by a k -complete component, the resulting graphs are denoted $C(k)$. The graph C we have considered so far will hence be referred to as graph $C(18)$ in the new notation.

The effects of changing d_{\max} by varying the size of the k -complete component in graphs $C(k)$ with $k \in \{3, \dots, 18\}$ are shown in Fig. 8. Figs. 8(a), (d) and (g) display plots of graphs $C(3)$, $C(10)$ and $C(18)$, respectively. Figs. 8(b), (e) and (h) show the eigengap bounds on the adjacency and unnormalised Laplacian normalised eigengaps corresponding to graphs $C(3)$, $C(10)$ and $C(18)$, respectively. Figs. 8(c), (f) and (i) show the two derived bounds (see Section IX-B) on the unnormalised and normalised Laplacian normalised eigengaps. Figs. 8(k) and (l) highlight the evolution of the eigengaps of the representation matrices as we vary k from 3 to 18; the eigengap markersize was chosen to increase with k to clearly show the evolution of the normalised eigengaps.

Note that the comparison of magnitudes of eigengaps corresponding to different representation matrices in Fig. 8 is sensible since we normalised all eigengaps by their spectral support and hence have all eigengaps on the same scale.

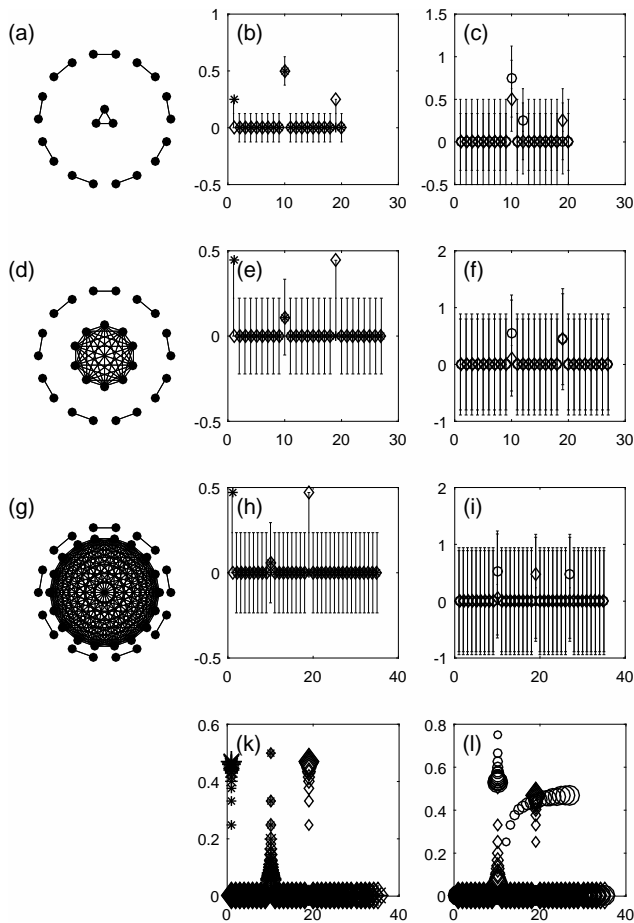


Fig. 8. Effects of changing d_{\max} by varying the size of the k -complete component in graphs $C(k)$ with $k \in \{3, \dots, 18\}$. (a), (d) and (g) contain plots of graphs $C(3)$, $C(10)$ and $C(18)$, respectively. (b), (e) and (h) bound $g(A, L)$ (shown via the intervals), together with the normalised eigengaps of the adjacency matrix $\mathcal{M}_i/\ell(\mu)$ (stars) and the normalised eigengaps of the Laplacian $\mathcal{L}_i/\ell(\lambda)$ (diamonds) corresponding to the graphs displayed at the start of their respective row of plots. (c), (f) and (i) bound $g'(L, L_{rw})$ (shown via inner intervals), bound $g(L, L_{rw})$ (via outer intervals), normalised eigengaps of the Laplacian $\mathcal{L}_i/\ell(\lambda)$ (diamonds) and normalised eigengaps of the normalised Laplacian $\mathcal{N}_i/\ell(\eta)$ (circles). (k) normalised eigengaps of the adjacency matrices (stars) and the normalised eigengaps of the Laplacian (diamonds) corresponding to graphs $C(k)$ with $k \in \{3, \dots, 18\}$. (l) normalised eigengaps of the Laplacian (diamonds) and the normalised eigengaps of the normalised Laplacian (circles) corresponding to graphs $C(k)$ with $k \in \{3, \dots, 18\}$. In plots (k) and (l) the marker size of the normalised eigengaps increases with growing k .

While significant differences in the spectra of A and L were observed in Fig. 7(a) of Section VIII-B, the eigengaps mostly agree (see Fig. 8(h)). Noticeably larger than other eigengaps are the first eigengap of the adjacency matrix, the 10th eigengap in both spectra and 19th eigengap in the unnormalised Laplacian spectrum. The spectra of A and L agree on the 10th eigengap, which is found to decrease with increasing d_{\max} in Fig. 8(k). The first and 19th eigengaps show clear disagreement between representation matrix spectra, and for these eigengaps the bound $g(A, L)$ can be seen to be tight on all three displayed examples, graphs $C(3)$, $C(10)$ and $C(18)$. The tightness of the bound here is due to the maximal crossover discussed in Section IX-A. Fig. 8(k) shows the difference in the eigengaps of the two representation matrices

growing with increasing degree extreme difference.

Turning now to Figs. 8(c), (f) and (g) it is seen that the difference between the two proposed bounds $g(L, L_{rw})$ and $g'(L, L_{rw})$ (Section IX-B), is rather small in this example and decreases as the degree extreme difference grows. The edges of the normalised eigengap bounds are not attained in Fig. 8. However, as discussed in Section VIII-A, this is not informative on the tightness of the bound, which is valid for *all elements* in the class of graphs $\mathcal{C}_{1,k}$; it is rather concerned with the particular structure of our examples. A feature of this comparison is the changing location of a notable eigengap, which is labelled as the $(k+9)$ th normalised eigengap present in the normalised Laplacian spectrum corresponding to graph $C(k)$. When clustering according to it in Section XI it will become apparent why the location of the gap is a function of k . From Fig. 8(l), as the degree extreme difference grows we find the difference of the $(k+9)$ th eigengaps of the two Laplacians to grow. In all of our examples, the $(k+9)$ th eigengap in the normalised Laplacian spectrum never overtakes the 10th eigengap, the only other notable eigengap. We would therefore recover the 10 connected components ahead of any other structure in the graph from the normalised Laplacian spectrum if we were to cluster according to the eigengaps in order of descending magnitude. For A and L this is only the case for small degree extreme differences as the 10th eigengap gets overtaken at $d_{\max} - d_{\min} = 3$ by the growing first eigengap in the adjacency spectrum and the growing 19th eigengap in the unnormalised Laplacian spectrum as seen in Fig. 8(k).

The disagreement of eigengap spectra highlights that the different representation matrices recover different structures of the graphs. The large first eigengap in the adjacency spectrum is understood as a measure of the connectedness of the graph and therefore, is seen to measure the increasing connectedness in the graph as the size of the fully connected component grows; nothing about clustering is necessarily indicated by the presence of the large first eigengap. The clustering structure suggested by the large 19th eigengap in the unnormalised Laplacian spectrum and the large 27th eigengap in the normalised Laplacian spectrum of graph $C(18)$ will be discussed in Section XI.

Remark 8: A further area of application for the bounds derived in this paper arises from a big data context. On large dataset the calculation of all three representation matrix spectra will come at a significant cost. However, calculating the bounds on normalised eigengap difference is inexpensive as it only requires calculation of the degree extremes, which are likely to be required at several stages of the graph's analysis. Using our inexpensive bounds practitioners will be able to anticipate the maximally different results they could have obtained using a different representation matrix. In Fig. 8(b) for example the 10th eigengap of the matrices is clearly bounded away from 0 and knowledge of any one of the two spectra would suffice to say with certainty that the other spectrum will also contain a significantly larger 10th eigengap than other eigengaps in the spectrum. \square

Remark 9: The examples of Fig. 8 show that the eigengap spectra of the three representation matrices can deviate significantly for several eigengaps, while approximately agreeing for

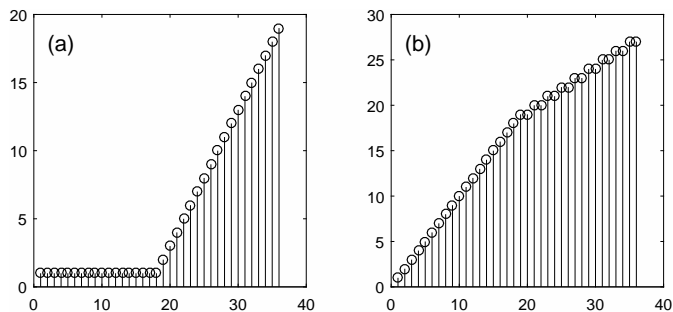


Fig. 9. (a) and (b) display the spectral clustering of graph $C(18)$ according to the first 19 eigenvectors of the unnormalised Laplacian L and the first 27 eigenvectors of the normalised Laplacian, respectively. The x-axes display a numbering of the 36 nodes in the graph; numbers 1 to 18 correspond to nodes in the 18-complete component and nodes 19-36 make up the 9 2-complete components. The y-axes display cluster indices ranging from 1 to 19 in (a) and 1 to 27 in (b).

the majority. We find these differences to increase with growing degree extreme differences as suggested by the functional form of our bounds. Since the large eigengaps in particular are commonly used to inform graphical analysis, a few large deviations in eigengap spectra can lead to significantly different inference as we will illustrate in Section XI. \square

XI. APPLICATION TO SPECTRAL CLUSTERING

We first cluster graph $C(18)$ according to the two large eigengaps which arose from the analysis in Section X. Then we discuss a clustering of the karate data set according to all three representation matrices. We find the choice of representation matrix to have a significant impact on the clustering outcome.

A. Spectral clustering of graph $C(18)$

We found that all representation matrices recover the 10 connected components perfectly when applying the spectral clustering algorithm to their respective first 10 eigenvectors. Additionally to the large tenth eigengap, we observed a large 19th eigengap in the *unnormalised* and a large 27th eigengap in the *normalised* Laplacian spectrum for graph $C(18)$ in Section X. At first sight it is unclear what structure is suggested by these eigengaps and hence we display the clustering according to the first 19 and 27 eigenvectors of the unnormalised and normalised Laplacians in Figs. 9(a) and (b), respectively.

From Fig. 9(a) we see that the large 19th eigengap in the unnormalised Laplacian eigengap spectrum suggests a clustering where the 18-complete component is recovered as a single cluster and the 9 2-complete components are treated as 18 individual clusters. From Fig. 9(b) we find that when clustering according to the first 27 eigenvectors of the normalised Laplacian we recover the 18-complete component as 18 clusters of one node each and each of the 2-complete components is exactly recovered. When varying $k \in \{1, \dots, 18\}$, the number of clusters in this clustering depends on the size of the k -complete component since each node in it is taken to be a separate cluster. This clarifies why

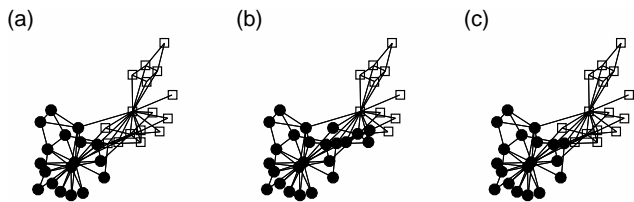


Fig. 10. Spectral clustering of the karate graph according to the first two eigenvectors of the adjacency matrix A in (a), the unnormalised Laplacian L in (b) and the normalised Laplacian L_{rw} in (c).

we observed the large $(k + 9)$ th eigengap in the normalised Laplacian spectrum as we varied k in Fig. 8.

Essentially, the two clusterings presented in Fig. 9 are complementary, in each case clustering all nodes of the same degree in one cluster and splitting the nodes of the remaining degree into separate clusters of single nodes.

The eigengaps, in conjunction with the spectral clustering algorithm, have revealed splits of the graphs, some of which might not have been anticipated.

B. Spectral clustering of the karate data set graph

To further illustrate the impact of the representation matrix choice, we display the spectral clustering according to the first two eigenvectors of each of the three representation matrices corresponding to the karate data set.

Since for the karate dataset, we have a reasonably large degree extreme difference, $d_{\max} - d_{\min} = 17$, we expect to see deviating results in the spectral clustering according to the different representation matrices.

At first sight, all clusterings displayed in Fig. 10 seem sensible. The clustering according to the two normalised Laplacians agrees and hence only one of the two is displayed. The clustering according to the adjacency matrix extends the cluster marked with the unfilled, square nodes by one node, karate club member 3, in comparison to the clustering according to the normalised Laplacian. In contrast, the unnormalised Laplacian detects 5 nodes less (karate club members 2, 4, 8, 14 and 20) in the cluster marked by the unfilled square nodes, than does the normalised Laplacian.

We find the clustering according to the adjacency matrix A to agree with the true clustering suggested by the eventual split of the karate club as recorded by [19]. The normalised Laplacians misplace one out of 34 nodes, which is known to be difficult to cluster correctly in the literature [8]. The unnormalised Laplacian however, misplaces 6 nodes, only one of which is known to us to be commonly misclustered. Hence, the unnormalised Laplacian clustering is clearly outperformed by the other two representation matrices when using the first two eigenvectors to find two communities in the karate data set. In [18] the conditions under which spectral clustering using the unnormalised Laplacian converges are shown to be more restrictive than the conditions under which spectral clustering according to the normalised Laplacian converges. [18] hence advocate using the normalised Laplacian for spectral clustering over the unnormalised Laplacian. Our clustering

results on graph $C(18)$ and the karate data set agree with this recommendation.

Remark 10: For our examples, the choice of representation matrix clearly impacts the results of cluster inference via spectral clustering. We suggest considering the degree extreme difference as a parameter in graphical signal processing to infer the potential impact of the choice of representation matrix. \square

XII. SUMMARY AND CONCLUSIONS

We have compared the spectra of the three graph representation matrices: the adjacency matrix A , the unnormalised graph Laplacian L and the normalised graph Laplacian L_{rw} and found differences in the spectra corresponding to general graphs. For all three pairs of representation matrices the degree extreme difference, $d_{\max} - d_{\min}$, was found to linearly upper bound the error when approximating eigenvalue spectra of one by an affine transformation of the spectrum of the other matrix. By considering the affine transformations we established correspondence of the largest adjacency eigenvalues to the smallest Laplacian eigenvalues. We explained the monotonicity found in the bounds by partitioning the class of graphs according to their degree extremes and considering the addition/deletion of connected components to/from the graph. The bounds were visualised on several graphs, including the literature standard Zachary's karate dataset, and the first bound $e(A, L)$ was found to be tight in two out of four examples. Finally, the bounds were extended to bound normalised eigengaps of the representation matrices. In examples with varying degree extremes, we saw that if the degree extreme difference is large, different choices of representation matrix may give rise to disparate inference drawn from graph signal processing algorithms; smaller degree extreme differences will result in consistent inference, whatever the choice of representation matrix. The significant differences in inference drawn from signal processing algorithms were visualised on the spectral clustering algorithm applied to model graphs and Zachary's karate graph. As a result of this work, we hope to have increased awareness about the importance of the choice of representation matrix for graph signal processing applications.

APPENDIX

A. Polynomial relation of representation matrix spectra

Here we will show that most matrix spectra can theoretically be exactly related via polynomial transforms and highlight practical issues with this approach.

The issue of mapping one set of representation matrix eigenvalues to another can be seen as a polynomial interpolation problem on the two sets of eigenvalues. [9, p. 390] state that as long as there exists a function which maps one set of input points to the set of output points, the interpolation problem always has a unique solution and they also provide formulas to find this solution. Therefore, we find that as long as equal eigenvalues in the domain are not required to be mapped to unequal eigenvalues in the range, there exists a unique polynomial which maps one representation matrix spectrum to another.

In practice, the operation of finding the interpolating polynomial can be numerically unstable and therefore while the polynomial mapping from one spectrum to another theoretically exists, it cannot be readily obtained. For example, for the graph of the real karate data set the interpolating polynomial maps eigenvalues $\mu_{13}, \dots, \mu_{22}$, which have a pairwise difference smaller than 10^{-14} onto eigenvalues of the unnormalised Laplacian which span an interval of width greater than 2. Obviously, finding the interpolating polynomial cannot be done without significant numerical error.

Furthermore, is it unclear how one would use the polynomial map between spectra for graphical inference. Relating the polynomial coefficients to vertex degrees could lead to great insight, but is hard to achieve. Finally, we are unaware of any results which would allow calculation of the transformation without calculating both representation spectra first, while our proposed affine transformation parameters only rely on the degree extremes which are readily available from the graph. Hence, while in theory, in some cases, there exists a more precise relation of the representation matrix spectra, our simple affine transformations have significant advantages.

B. Weyl's inequality and the bound of (6)

In (2) of Section II we define $\hat{L} = L + d_1 I - D$. Denote the error between \hat{L} and L by $\Delta = d_1 I - D$, and the error eigenvalues as follows: $\lambda_1(\Delta) \leq \lambda_2(\Delta) \leq \dots \leq \lambda_n(\Delta)$. Weyl's inequality states that, for $i \in \{1, 2, \dots, n\}$,

$$\lambda_i + \lambda_1(\Delta) \leq \lambda_i(\hat{L}) \leq \lambda_i + \lambda_n(\Delta).$$

So, in particular,

$$\begin{aligned} \lambda_1(\Delta) &\leq \lambda_i(\hat{L}) - \lambda_i \leq \lambda_n(\Delta) \\ \Rightarrow d_1 - d_{\max} &\leq \lambda_i(\hat{L}) - \lambda_i \leq d_1 - d_{\min}. \end{aligned}$$

Now, set $d_1 = (d_{\max} + d_{\min})/2$ to obtain the result derived in (6) of Section II, which is a bound on the absolute difference.

This result extends the application of Weyl's inequality to the two representation matrix spectra, as is done in [16, p. 71], by transforming one of the two spectra.

C. Choosing c_2

In what follows we refer to the terms $|c_2|(d_{\max} - d_{\min})/2$ and $2 \max(|d_{\max}c_2 - 1|, |d_{\min}c_2 - 1|)$ as term 1 and term 2, respectively. We proceed by analysing the bound in the three different intervals

$$\left(-\infty, 0\right), \left[0, \frac{2}{d_{\max} + d_{\min}}\right], \left(\frac{2}{d_{\max} + d_{\min}}, \infty\right).$$

For $c_2 \in \left(-\infty, 0\right)$ we have,

$$\max(|d_{\max}c_2 - 1|, |d_{\min}c_2 - 1|) = -d_{\max}c_2 + 1,$$

and both terms 1 and 2 decrease as c_2 increases. Hence, the overall bound is decreasing and thus, the value of c_2 minimising the bound, satisfies $0 \leq c_2$.

For $c_2 \in \left(2/(d_{\max} + d_{\min}), \infty\right)$ we have

$$\max(|d_{\max}c_2 - 1|, |d_{\min}c_2 - 1|) = d_{\max}c_2 - 1.$$

Hence, both terms 1 and 2 are increasing, and the value of c_2 minimising the bound satisfies $c_2 \leq 2/(d_{\max} + d_{\min})$.

Finally, for $c_2 \in [0, 2/(d_{\max} + d_{\min})]$, we have

$$\max(|d_{\max}c_2 - 1|, |d_{\min}c_2 - 1|) = -d_{\min}c_2 + 1.$$

Hence, term 2 is decreasing while term 1 is increasing. We will now determine which of the two terms defines the monotonicity of the bound by comparing slopes.

$$\begin{aligned} \text{Term 1 dominates term 2} &\iff \frac{d_{\max} - d_{\min}}{2} - 2d_{\min} > 0 \\ &\iff d_{\max} > 5d_{\min}. \end{aligned}$$

Hence, if $d_{\max} > 5d_{\min}$, the bound is increasing in the interval $[0, 2/(d_{\max} + d_{\min})]$. Therefore, $c_2 = 0$ minimises the bound, so that

$$\begin{aligned} |\eta_i(\tilde{L}_{rw}) - \eta_i| &\leq \left(|c_2| \frac{d_{\max} - d_{\min}}{2} \right. \\ &\quad \left. + 2 \max(|d_{\max}c_2 - 1|, |d_{\min}c_2 - 1|) \right)_{c_2=0} \\ &= 2 \text{ for } d_{\max} > 5d_{\min}. \end{aligned} \quad (32)$$

Otherwise, if $d_{\max} \leq 5d_{\min}$, we have a decreasing bound. This results in a minimal bound at $c_2 = 2/(d_{\max} + d_{\min})$ and the bound value

$$\begin{aligned} |\eta_i(\tilde{L}_{rw}) - \eta_i| &< \left(|c_2| \frac{d_{\max} - d_{\min}}{2} \right. \\ &\quad \left. + 2 \max(|d_{\max}c_2 - 1|, |d_{\min}c_2 - 1|) \right)_{c_2 = \frac{2}{d_{\max} + d_{\min}}} \\ &= \frac{d_{\max} - d_{\min}}{d_{\max} + d_{\min}} + 2 \frac{d_{\max} - d_{\min}}{d_{\max} + d_{\min}} \end{aligned} \quad (33)$$

$$= 3 \frac{d_{\max} - d_{\min}}{d_{\max} + d_{\min}} \leq 2 \text{ for } d_{\max} \leq 5d_{\min}. \quad (34)$$

The result in (33) follows from plugging c_2 into term 1 and recognising that term 2 is degenerate since both its arguments are equal. We denote the resulting bound by $e'(A, L_{rw})$:

$$e'(A, L_{rw}) \stackrel{\text{def}}{=} \begin{cases} 3 \frac{d_{\max} - d_{\min}}{d_{\max} + d_{\min}}, & \text{for } d_{\max} < 5d_{\min}; \\ 2, & \text{otherwise.} \end{cases} \quad (35)$$

For d -regular graphs, for which $d_{\max} = d_{\min} = d$, the upper result applies, and we see that the bound is again zero. For a graph with disconnected nodes $d_{\min} = 0$, the lower result applies, and the bound is 2; from (34) this is the maximal bound and unlike when comparing L and L_{rw} , this bound is already reached for $d_{\max} \geq 5d_{\min}$, and not in the limit $d_{\max} \rightarrow \infty$ for fixed d_{\min} .

From (13) we see that if $c_2 = 0$, then the transformation is degenerate, non-invertible and all information is lost in the process. Hence we will reject the bound value $e'(A, L_{rw}) = 2$ for $d_{\max} > 5d_{\min}$ even though it results in the minimal bound value – the lowest bound value achieved under our analysis framework and not the absolute minimal bound, i.e., a tight bound. So, we adopt the bound given in (18), namely,

$$e(A, L_{rw}) \stackrel{\text{def}}{=} 3 \frac{d_{\max} - d_{\min}}{d_{\max} + d_{\min}}.$$

ACKNOWLEDGMENT

The work of Johannes Lutzeyer is supported by the EPSRC (UK).

REFERENCES

- [1] Z. Bai, J. Demmel, J. Dongarra, A. Ruhe & H. van der Vorst. *Templates for the solution of algebraic eigenvalue problems: a practical guide*. SIAM, 2000.
- [2] V. Batagelj and A. Mrvar, ‘‘Pajek datasets,’’ <http://vlado.fmf.uni-lj.si/pub/networks/data/>. 2006. Accessed: 2016-11-23
- [3] D. S. Bernstein, *Matrix Mathematics: Theory, Facts, and Formulas (2nd Edition)*. Princeton, NJ: Princeton University Press, 2009.
- [4] P. J. Bickel & S. Purnmarita, ‘‘Hypothesis testing for automated community detection in networks,’’ *J. Royal Statistical Society B*, vol. 78, pp. 253–273, 2016.
- [5] P.-Y. Chen & A. Hero, ‘‘Deep community detection,’’ *IEEE Transactions on Signal Processing*, vol. 63, pp. 5706–5719, 2015.
- [6] F. R. K. Chung, *Spectral Graph Theory*, Providence, RI: American Mathematical Soc., 1997.
- [7] D. Cvetkovic & I. Gutman, ‘‘Applications of graph spectra: An introduction to the literature,’’ *Zbornik radova*, vol. 14, pp. 9–34, 2011.
- [8] S. Fortunato, ‘‘Community detection in graphs,’’ *Physics Reports*, vol. 486, pp. 75–174, 2010.
- [9] R. A. Horn & C. R. Johnson, *Topics in Matrix Analysis*, Cambridge U.K., Cambridge University Press, 1991.
- [10] B. Karrer & M. E. J. Newman, ‘‘Stochastic blockmodels and community structure in networks,’’ *Physical Review E*, vol. 83, 016107, 2011.
- [11] J. Lei & A. Rinaldo, ‘‘Consistency of spectral clustering in stochastic block models,’’ *The Annals of Statistics*, vol. 43, pp. 215–237, 2015.
- [12] K. Rohe, S. Chatterjee & B. Yu, ‘‘Spectral clustering and the high-dimensional stochastic blockmodel,’’ *The Annals of Statistics*, vol. 39, pp. 1878–1915, 2011.
- [13] A. Sandryhaila, & J. M. F. Moura, ‘‘Big data analysis with signal processing on graphs: Representation and processing of massive data sets with irregular structure,’’ *IEEE Signal Processing Magazine*, vol. 31, pp. 80–90, 2014.
- [14] D. Shuman, S. K. Narang, P. Frossard, A. Ortega & P. Vandergheynst, ‘‘The emerging field of signal processing on graphs: Extending high-dimensional data analysis to networks and other irregular domains,’’ *IEEE Signal Processing Magazine*, vol. 30, pp. 83–98, 2013.
- [15] N. Tremblay, & P. Borgnat, ‘‘Graph wavelets for multiscale community mining,’’ *IEEE Signal Processing Magazine*, vol. 62, pp. 5227–5239, 2014.
- [16] P. van Mieghem, *Graph Spectra for Complex Networks*, Cambridge U.K., Cambridge University Press, 2011.
- [17] U. von Luxburg, ‘‘A tutorial on spectral clustering,’’ *Statistics and Computing*, vol. 17, pp. 395–416, 2007.
- [18] U. von Luxburg, M. Belkin & O. Bousquet, ‘‘Consistency of spectral clustering,’’ *The Annals of Statistics*, vol. 36, pp. 555–586, 2008.
- [19] W. W. Zachary, ‘‘An information flow model for conflict and fission in small groups,’’ *Journal of Anthropological Research*, vol. 33, pp. 452–473, 1977.